SPIE Proceedings: Style template and guidelines for authors

Anna A. Author[a] and Barry B. Author[b]

[a]Affiliation1, Address, City, Country
[b]Affiliation2, Address, City, Country

ABSTRACT

This document is prepared using LaTeX2e[1] and shows the desired format and appearance of a manuscript prepared for the Proceedings of the SPIE.* It contains general formatting instructions and hints about how to use LaTeX. The LaTeX source file that produced this document, `article.tex` (Version 3.4), provides a template, used in conjunction with `spie.cls` (Version 3.4). These files are available on the Internet at `https://www.overleaf.com`. The font used throughout is the LaTeX default font, Computer Modern Roman, which is equivalent to the Times Roman font available on many systems.

Keywords: Manuscript format, template, SPIE Proceedings, LaTeX

1. INTRODUCTION

The Gamma Ray bursts are transient celestial events that are thought to be produced by the collapse of massive stars or by the coalescence of two compact objects. Their main observational characteristics are the huge luminosity and fast variability, often as short as one millisecond, with a spectral emission localized between the hard X-rays and soft Gamma rays. This phenomena have duration that can vary in each case, starting from few decimals of seconds up to hundreds of seconds. For this reason the GRBs population is catalogued according to the time scale during which the 90% of the flux is emitted by the source (F_{90}). The population of Short GRBs includes bursts with $T_{90} \lesssim 2$ s, whilst GRBs with larger values of T_{90} are catalogues as Long GRBs. Assuming isotropic emission the energy released can attain 10^{54} erg, i. e. the rest mass energy of the Sun (see e.g. Bloom et al. 2009, ApJ, 691, 723), in about 100s duration. However it is now believed that strong beaming reduces the energetic budget up to three orders of magnitude (Abdo et al. 2009, Science, 323, 1688).
The coalescence of compact objects, neutron stars (NS) and black holes (BH), and the sudden collapse to form a BH, are fundamental to investigate both the physics of matter under extreme conditions, and the ultimate structure of space-time. For this reason, a fast and accurate localization of the prompt emission of the GRBs is fundamental, especially for the syncronous observation of the GRB phenomenology with different observatories. In this work we investigate on the position accuracy that can be reached using a couple of mini-satellites of the *HERMES* swarm. The spatial localization of the events can be estimated taking advantage from the direct measurement of the photon arrival times in each detector and then by an estimation of the photons arrival times that can be obtained by a cross-correlation analysis. In the hypothesis of GRB whose emitted photons arrive to a series of N detectors uniformly distibuted in an orbit, the positional accuracy that can be obtained is given by:

$$\sigma_{pos} = \frac{(E_{cc} + E_{pos} + E_{time})^2}{< Baseline > \sqrt{(N-1-2)}} \tag{1}$$

where E_{cc} is the error on the delay time given by the cross-correlation between the light-curves recorded by two detectors, E_{POS} is the error induced by the uncertainty in the space localisation of the detectors, E_{time} is the error on the absolute time reconstruction, $< Baseline >$ is the average distance between the detectors ad $N_{ind} = N - 1$ is the number of statistically independent couples of satellites.
This relation highlights how the positional accuracy, in addition to the number of satellites making up the swarm, is strongly dependent from the uncertainty on the cross-correlation delay measurement E_{cc}. In order to obtain a realistic estimation of this uncertainty as a function of the GRB duration, flux and of its intrinsic variability, we have to take advantage of the current repositories of both short and long GRB data, in order to simulate as much as possible the wide phenomenological properties characterizing these transient events, as seen by the future *HERMES* mission.

Further author information: (Send correspondence to A.A.A.)
A.A.A.: E-mail: aaa@tbk2.edu, Telephone: 1 505 123 1234
B.B.A.: E-mail: bba@cmp.com, Telephone: +33 (0)1 98 76 54 32
*The basic format was developed in 1995 by Rick Hermann (SPIE) and Ken Hanson (Los Alamos National Lab.).

2. DATA ANALYSIS

One of the most performant GRB monitors currently on orbit is part of the *Fermi* mission, launched on June 11th 2008. The *Fermi* Gamma-ray Space Telescope explores energetic and transient phenomena in an energy range that is included between 10 keV and 300 GeV. It consists of the Large Area Telescope (*LAT*) and of the Gamma-ray Burst Monitor (*GBM*). The first instrument observes in the energy range 20 MeV 300 GeV with a maximum effective area of about 8000 cm^2. The *GBM*, on the other hand, consists of two different kinds of detectors: twelve sodium iodide (NaI) scintillators and two cylindrical bismuth germanate (BGO) scintillators, both having a collecting area of about 125 cm^2. The NaI detectors are sensitive to energies included between few keV up to about 1 MeV, while the BGO detectors cover the energy range 150 keV to 30 MeV. The triggering process of *GBM* starts when a significant change in count-rate due to an event is recorded in at least two of the NaI scintillators. In addition, data captured with the so called *Time-tagged event (TTE)* format, can continuously be recorded with a time resolution of $2\mu s$ to provide about 15-30 s of pre-trigger information for each GRB and about 300 s of data after the trigger time. Due to the good time resolution provided by this instrument, the *TTE* data represent a powerful mean for studying the performances of the *HERMES* mission.
HERMES will consist of a swarm of cubesats that will equipped with scintillators that will be nominally be sentitive to the energy range 50 keV - 300 keV. For this reason each observation of the *GBM* has been previously filtered in order to have events only in this energy range.

The aim of this work is to test the accuracy in detecting the delays of the GRBs photon arrival times in a couple of detectors via cross-correlation techniques. For this reason, the *GBM* light curves opportunely processed will be fundamental to simulate light curves of a sample of GRB using Montecarlo simulations. These curves will be cross-correlated in order to obtain a cross-correlation profile from which the delay will be measured as shown in the following.

In order to simulate the cross correlation profiles of the burst as seen by *HERMES*, we have first to build a functional model describing the observed profile of the event; this model will be hereafter called *GRB template*. In order to produce the template for each analysed GRB, we followed some precise steps that we report in the following.
The cross correlation of light curves with extremely small bin time are considerable challenging due to the fact that the statistics of the detection processes is essentially Poissonian, and for this reason the fluctuations in each bin with respect to the expected counts are of the order of the 100%, especially for weak sources. This is a relevant problem when we try to amplify the signal of the source to take into account a specific effective area to simulate for the detector. We found a partial solution to this problem adopting time bins in the light curves that are characterized by a constant number of counts. In particular, we rebinned each light curve defining a temporal bin every time 6 counts were collected; this technique actually provides a preservation of the variability of the signal, introducing fluctuations that are not larger than the 30%.
The curves we obtain in this way shows uneven bins and for this reason these needs to be processed in order to be used with different bin times. Then, we performed a linear interpolation of the counts on the uneven bin light curve and rebinned each obtained curve with the bin time we want to use for our work. In addition, before and after the burst, where only background noise is collected by the detector, we considered to evaluate the mean value of the counts that and to replace this value to the actual signal. This step will be useful to speed up the Montecarlo simulation of the light curves of the source and it is based on the fact that the cross correlation of random noise due to the background contribution before and after the GRB is flat. The obtained curve is the template of the GRB we want to simulate and it is shown in Figure 1 for the case of the long GRB 130502327 and of the short GRB 120323507.

Each template represents the model of the GRB we want to simulate, and for this reason it will be used to simulate the light curves observed by each couple of detectors we want to consider. In order to simulate detectors with different overall effective areas, each template has been amplified by a constant factor k that is equal to $k = A_{sim}/A_{GBM}$, where A_{sim} and A_{GBM} are the areas we want to simulate and that of *GBM*, respectively. The Montecarlo simulations of the light curves of each GRB are successively performed with a Poissonian randomization of the counts contained in each bin of the template. The obtained couple of light curves is then cross-correlated in order to highlight the injected time delay between the curves. In our case, we did not injected a delay between the two signals, then simulating the case in which the couple of detectors is located in the same plane.
The obtained cross correlation profiles are extremely different between each other. The length of the signal is equivalent to the total duration of the analysed light curves but the shape but its variability is strongly related to the complexity of the

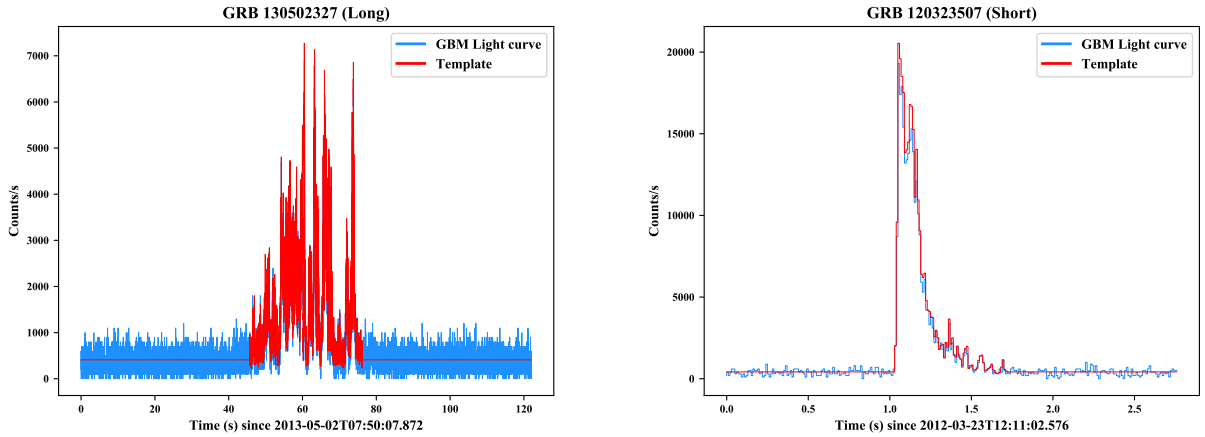

Figure 1. The Fermi/GBM light curves of the long GRB 130502327 and of the short GRB 120323507 and the relative *template* obtained with the procedure described in the text. In both cases, for reasons of clarity, we used a bin time of 10^{-2} s for the light curves and templates of both the GRBs.

input light curves and to their intrinsic time variability, as visible in Figure 2. The main peak of this profile returns the value of the time delay for which the pair of input light curves match as much as possible. To obtain the value of this delay, we fitted each profile with an 'ad hoc' function in a limited range of delays around the peak. In the insets of Figure 2, for example, we report a zoom of the peak of the cross-correlation obtained for the long GRB 130502327 and for the short GRB 120323507. In both these cases, this limited part of the cross correlation profile has been fitted with a Gaussian function (red solid line), where the value of the centroid represents the time delay between the light curves collected by the two detectors.

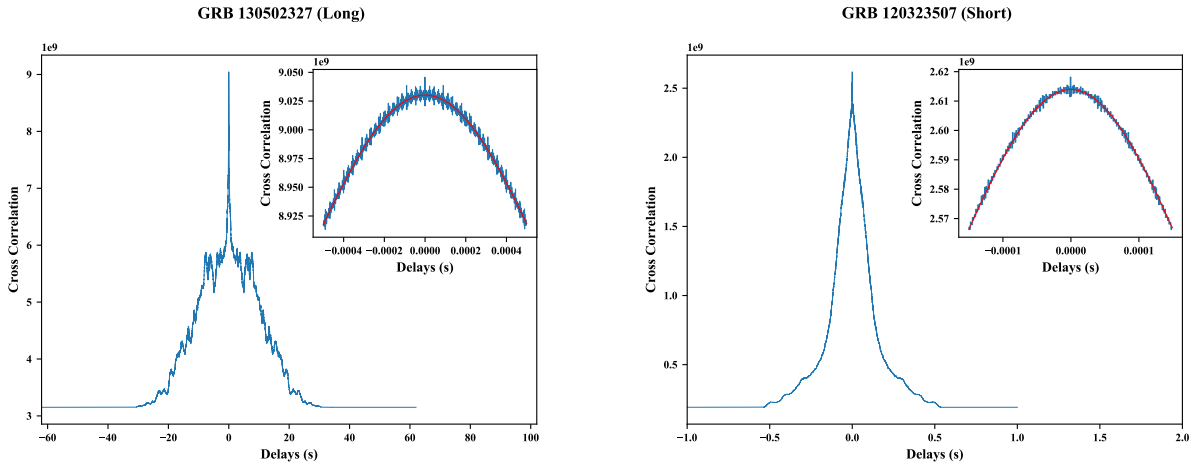

Figure 2. The Cross correlation profiles obtained by simulating the Fermi/GBM light curves of the long GRB 130502327 and of the short GRB 120323507 using the templates shown in Figure 1 for each burst. In each panel we also report an inset showing a zoom of the cross correlation profiles around the peak, and the best fit function resulting by fitting the cross correlation profile in this region with a Gaussian function (red solid line). For the reported cross correlation profiles we used a bin time of $1\mu s$.

In order to investigate how the accuracy of the measurement for a certain burst is statistically distributed we have to perform Montecarlo simulations of a large number of light curves, as they were collected by detectors with a given collecting area. In addition, it is also considerably interesting to investigate on how this accuracy depends on the area of the detectors, considering both long and short GRBs.
For this reason, we selected a sample of 100 long and short GRBs from the Fermi/GBM archive and chose to perform the

analysis taking into account six different areas to simulate for the couple of the detectors: 100 m^2, 50 m^2, 10 m^2, 1 m^2, 0.0125 m^2 (i.e the *GBM* effective area) and 0.0056 m^2 (i.e. the expected area of each HERMES nano-sat).
The sample of GRB we chose is absolutely casual and for this reason is absolutely rapresentative of the wide variety of phenomenologies, fluxes, durations and intrinsic variability that were recorded during the Fermi mission up to the moment in which this paper was written. For the long GRBs we selected bursts having net fluxes ranging between 0.16 and 26 ph cm^{-2} s^{-1}, durations of the bursts between 3 and 138 s, and fluences between 1.67 and 4 ph cm^{-2}. On the other hands, we selected short GRBs with net fluxes between 0.6 and 188 ph cm^{-2} s^{-1}, durations between 0.03 and 1.9 s and fluences between 0.2 and 75 ph cm^{-2}. Just for comparison, in all the *GBM* observations the average value of the background flux is of about 3 ph cm^{-2} s^{-1}.
For each selected burst, and for each considered area we simulated 1000 cross correlation curves (i.e. 1000 couples of light curves of the burst). For each cross correlation profile, as previously shown, we found the injected value of the delay by fitting the peak region with a function that in turn was chosen between a Gaussian function, a composite function consisting in two Gaussian profiles having a common centroid but different σ, a Gaussian function plus an asymmetric double exponential function or alternatively a pure asymmetric double exponential function. Depending on the particular shape of the cross correlation profile we chose that function between those listed for which the fit returned the minimum χ^2 value. This analysis has been repeated for both the samples of GRBs (long and short) and for all the considered areas and consisted in 1.2×10^6 couples of simulated light curves from which we obtained the same number of cross correlation profiles, with an overall substantial computational effort that required high storage and computational performances in a multi-core server of 144 logical processors and 504 Gb of RAM.

3. DISCUSSION

To obtain a realistic estimation of the accuracy that can be achieved in the measurement of the delays of the arrival times for photons emitted by GRBs in two detectors, we built a method with which we simulated several light curves of different kinds of GRBs. From a cross correlation of each couple of curves we obtained a measurement of the delay between the two signals that was obtained by fitting the peak of the cross correlation profile with an opportune function.
With a so large sample of GRBs events analysed, a good estimation of the accuracy in determining the delays is given by measuring how for a given typology of burst (long or short) and for each simulated area the centroids distributes around the value of the injected delay. We show the distributions obtained for the long GRB 130502327 and for the short GRB 120323507 in Figure 3. Each delay distribution was fitted with a Normal distribution that allowed to infer a realistic estimation of the delay injected in the simulated light curves and of the dispersion of the delay measurements with respect to the expected value, i.e. a realistic estimation of the cross correlation error E_{cc} defined in Equation 1. This analysis has been repeated for the whole set of areas we simulated and for both the long and short GRBs. In addition, we also compared the mean cross correlation error $< \sigma >$ obtained from the analysis of the delay distributions with the mean value $< \epsilon >$ of the error associated to the centroid obtained from the fit of the cross correlation peak region. We report the results of this analysis in Table 3 and Figure 3 for the long and short data sets of GRBs. From these results it is evident how adopting the ϵ error underestimates the error on the delay measurement via the cross correlation profile, hence resulting in an overestimation of the accuracy in the position of the GRB. In particular, the ratio $< \sigma > / < \epsilon >$ decreases with decreasing the area of the detector as a consequence of the decrement of the statistics of the data collected by smaller areas. For the same reason it is evident how the mean value of σ increases with decreasing the detector area.

More precisely, it is interesting to notice the trend followed by the σ inferred by the fit of the cross correlation profile as a function of the fluence of the GRBs for each simulated area. In Figure 4 and Figure 5 we report these trends for the long and short GRBs considered in our work, respectively. From a quick comparison between the plots in the two figures it can be evinced that the high statistics that can be achieved by the long GRBs, in addition to that characterizing the higher simulated areas for the short GRBs, allows to obtain a more defined profile for the trends, due to the better constraints obtained for the delay measurement in the cross correlation profile. On the contrary, the lower areas, especially for the short GRBs, implied a scattered distribution of the data. However, in both the cases it can be inferred that the error σ on the delay measurement decreases with increasing the fluence of the considered GRB, as a consequence of the increase in the statistics of the data.
We modelled these trends using a functional form as $y(x) = a + bx^k$, where k is a power included between -1 and -0.001. We performed a fit for each k at steps of $\delta k = 1 \times 10^{-4}$ for a total of 9990 fits for each simulated area and GRB typology

	Long GRBs			
Area (m^2)	k	a	b	$\chi^2(d.o.f)$
100	-0.2	-56(10)×10^{-7}	20(2)×10^{-6}	5.4×10^{-10}(98)
50	-0.322	-38(6)×10^{-7}	29(2)×10^{-6}	6×10^{-10}(98)
10	-0.216	-134(8)×10^{-7}	49(2)×10^{-6}	4.5×10^{-10}(98)
1	-0.256	-27(2)×10^{-6}	133(5)×10^{-6}	4.3×10^{-9}(98)
0.0125	-0.313	-44(4)×10^{-5}	279(10)×10^{-5}	2×10^{-6}(98)
0.0056	-0.608	-18(7)×10^{-5}	102(4)×10^{-4}	3×10^{-5}(98)

Table 1. Best-fit models obtained by fitting the long GRBs σ vs. fluence profiles with the functional form $y(x) = a + bx^k$. The errors associated to the parameters were evaluated at a confidence level of the 68%.

	Short GRBs			
Area (m^2)	k	a	b	$\chi^2(d.o.f)$
100	-0.304	-57(11)×10^{-7}	159(14)×10^{-7}	8.4×10^{-10}(98)
50	-0.303	-8(2)×10^{-6}	23(2)×10^{-6}	2×10^{-9}(98)
10	-0.325	-17(3)×10^{-6}	49(4)×10^{-6}	8×10^{-9}(98)
1	-0.327	-56(11)×10^{-6}	160(14)×10^{-6}	1×10^{-7}(98)
0.0125	-0.164	-0.011(3)	0.018(3)	0.002(98)
0.0056	-0.010	-0.50(14)	0.52(15)	0.02(98)

Table 2. Best-fit models obtained by fitting the short GRBs σ vs. fluence profiles with the functional form $y(x) = a + bx^k$. The errors associated to the parameters were evaluated at a confidence level of the 68%.

(long or short); we chose as best-fit function the one having a k for which, together with the a and b parameters, we obtain a minimum of the χ^2. On average, we obtained a minimum of the χ^2 for $k = -0.32$ for all the areas and both for the long and short GRBs, not considering the values of k obtained for the areas 0.0125 m^2 and 0.0056 m^2 simulated for the short GRBs, for which we obtain a considerably flat power of -0.16 and -0.01, respectively, due to the scattered profiles in these two cases. We report the obtained fit parameters in section 3 and Table 3.

ACKNOWLEDGMENTS

This unnumbered section is used to identify those who have aided the authors in understanding or accomplishing the work presented and to acknowledge sources of funding.

REFERENCES

[1] Lamport, L., [*LaTeX: A Document Preparation System*], Addison-Wesley, Reading, Mass. (1994).

	Short GRBs			
Area (m^2)	σ_{min}	σ_{max}	$< \sigma >$	$< \sigma >/< \epsilon >$
100	5.974907063724057e-08	1.8347673286588637e-05	6.534330112671629e-06	7.3457365782627235
50	8.327817977413326e-08	2.8146661479250482e-05	9.21619292355443e-06	6.200167445616318
10	1.867258872028386e-07	6.102888687738298e-05	2.0331103734181935e-05	6.701879256463874
1	5.771539436685253e-07	0.00021081777428695462	6.453042063262608e-05	5.039805652851995
0.0125	9.560084714842066e-06	0.025972208446171898	0.004584209602272932	4.294325462320192
0.0056	1.9398674274012946e-05	0.0787462424572527	0.01360441039839945	4.811604623009573

Table 3. Resume of the results obtained from the simulation of a sample of 100 Short GRBs from the Fermi/GBM archive as a function of the simulated collecting area.

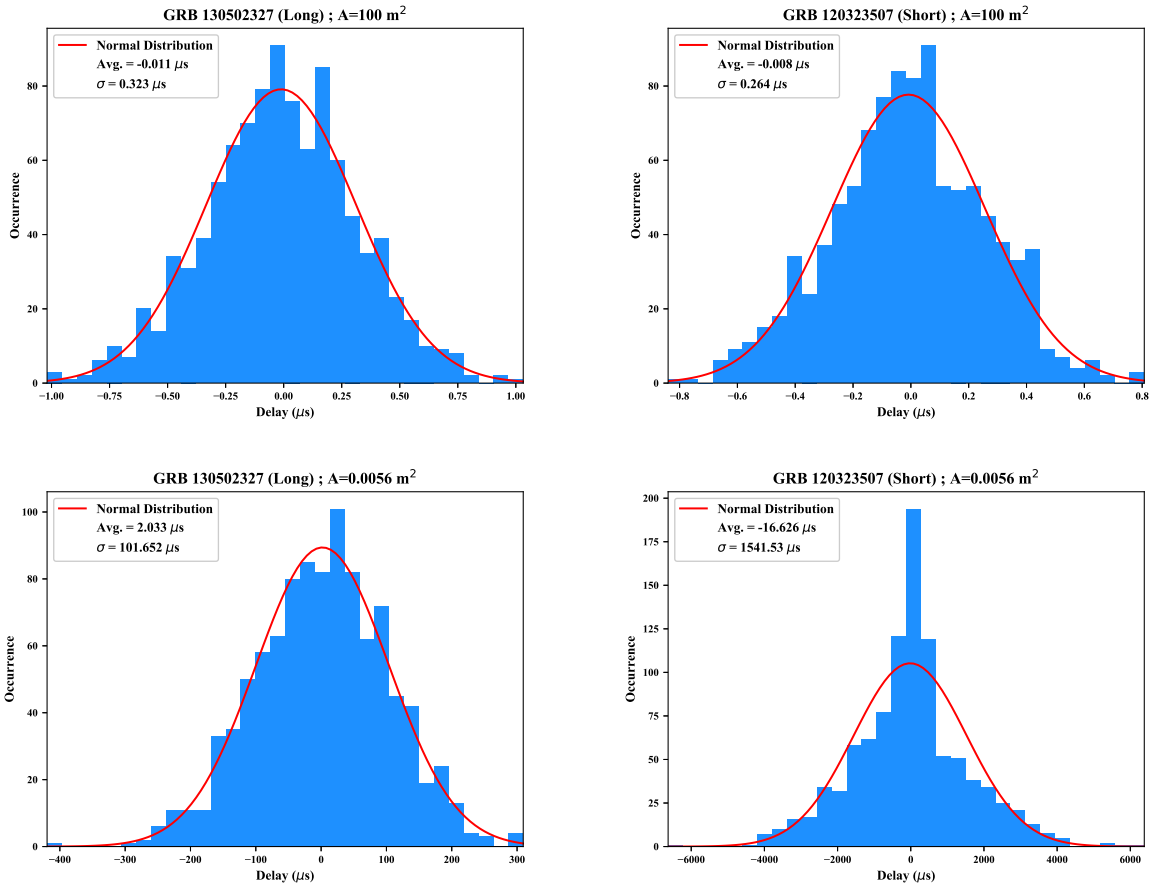

Figure 3. Distributions of the delays obtained for the long GRB 130502327 (left column) and the short GRB 120323507 (right column). For each burst we show a comparison between the results obtained for a simulated area of 100 m^2 (on the top) and of 0.0056 m^2 (on the bottom).

	Long GRBs			
Area (m^2)	σ_{min}	σ_{max}	$< \sigma >$	$< \sigma > / < \epsilon >$
100	1.2288202791919088e-07	1.3893084036386532e-05	4.421738574898745e-06	5.163571094402115
50	1.7357168814420108e-07	2.0104233385850118e-05	5.669313287935561e-06	3.2135421748743354
10	3.987123355230972e-07	2.5728427221454894e-05	9.320900692181446e-06	3.2093913438856703
1	1.3132966330242298e-06	7.713557028223853e-05	2.6879835390663862e-05	2.8811619807648956
0.0125	1.798680374494856e-05	0.001739569989617569	0.0004975834853598062	1.3351867706734453
0.0056	3.4300685103588634e-05	0.0063206606110297586	0.001209711899944309	1.252797733846769

Table 4. Resume of the results obtained from the simulation of a sample of 100 Long GRBs from the Fermi/GBM archive as a function of the simulated collecting area.

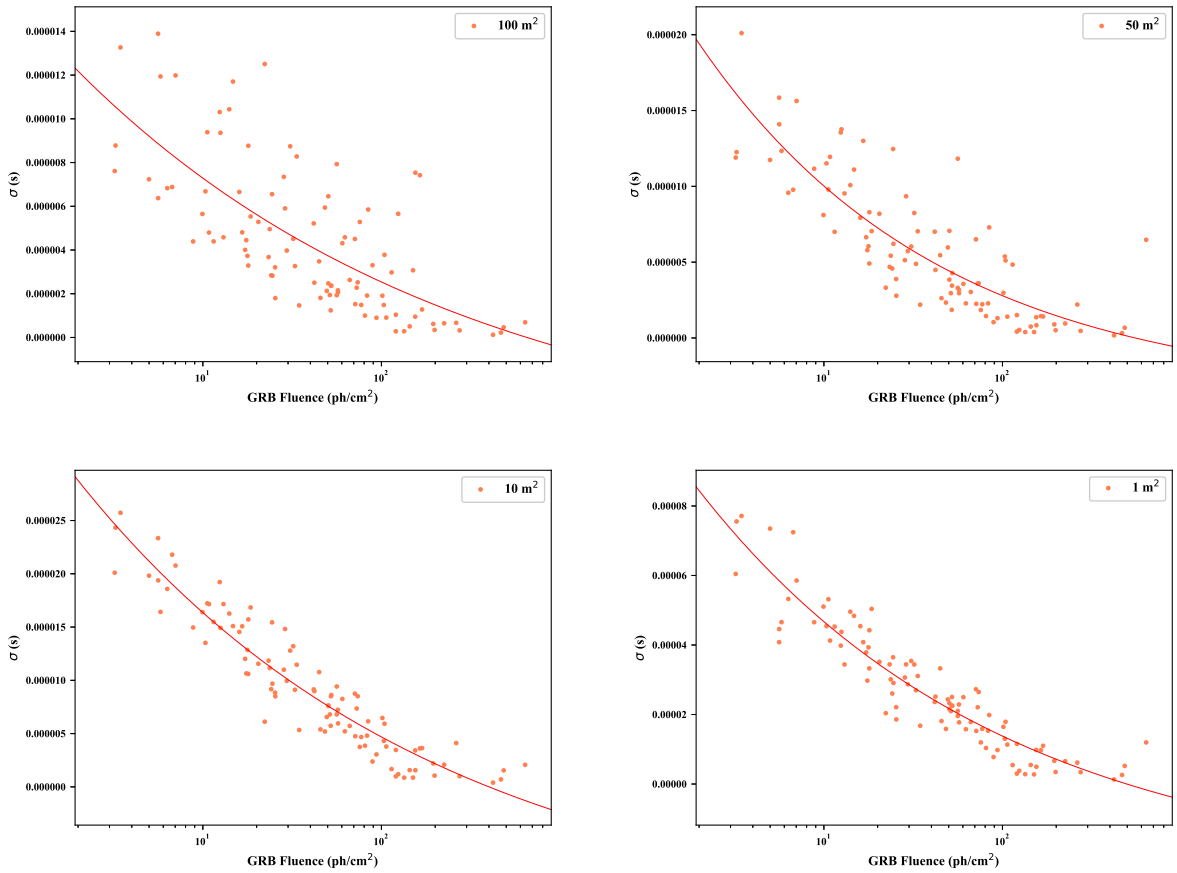

Figure 4. σ of the centroids distribution obtained from the cross correlation curves of the long GRBs, as a function of the GRB fluence for each simulated area. The red solid lines represent the best-fit functions $y(x) = a + bx^k$, where k is the power that minimizes the χ^2, together with the parameters a and b (see section 3 and Table 3 for the parameters obtained for the long and short GRBs, respectively).

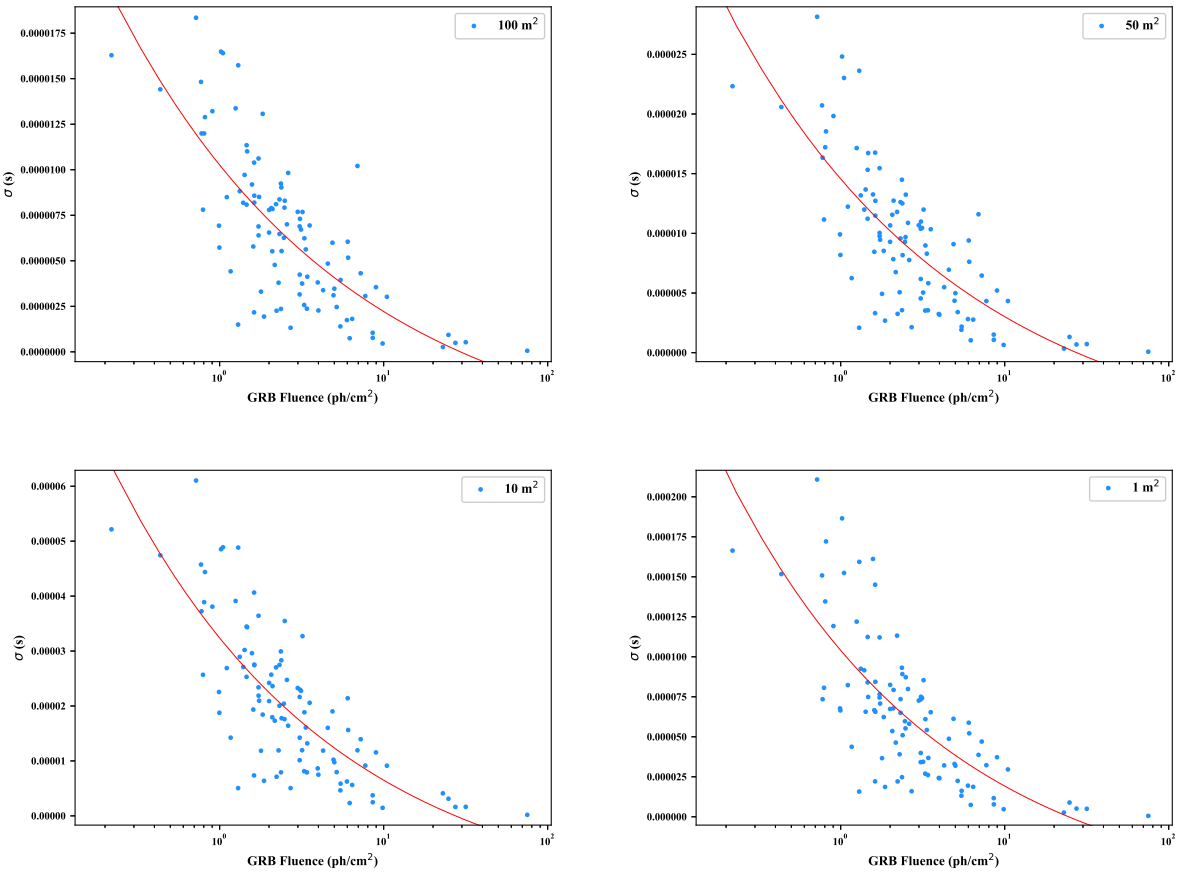

Figure 5. σ of the centroids distribution obtained from the cross correlation curves of the short GRBs, as a function of the GRB fluence for each simulated area. The red solid lines represent the best-fit functions $y(x) = a + bx^k$, where k is the power that minimizes the χ^2, together with the parameters a and b (see section 3 and Table 3 for the parameters obtained for the long and short GRBs, respectively).

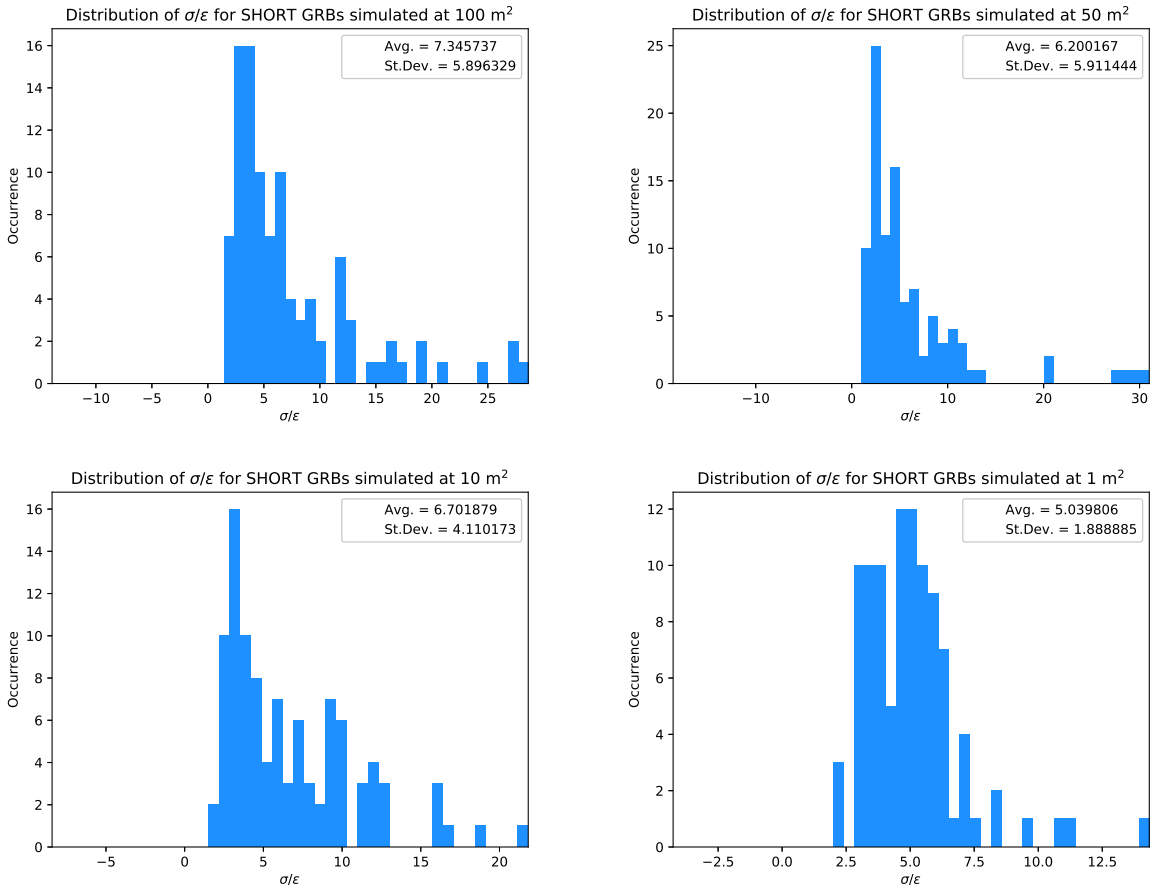
Distribution of σ/ε for SHORT GRBs simulated at 100 m²
Avg. = 7.345737
St.Dev. = 5.896329
Occurrence
σ/ε
Distribution of σ/ε for SHORT GRBs simulated at 50 m²
Avg. = 6.200167
St.Dev. = 5.911444
Occurrence
σ/ε
Distribution of σ/ε for SHORT GRBs simulated at 10 m²
Avg. = 6.701879
St.Dev. = 4.110173
Occurrence
σ/ε
Distribution of σ/ε for SHORT GRBs simulated at 1 m²
Avg. = 5.039806
St.Dev. = 1.888885
Occurrence
σ/ε

Figure 6. ...

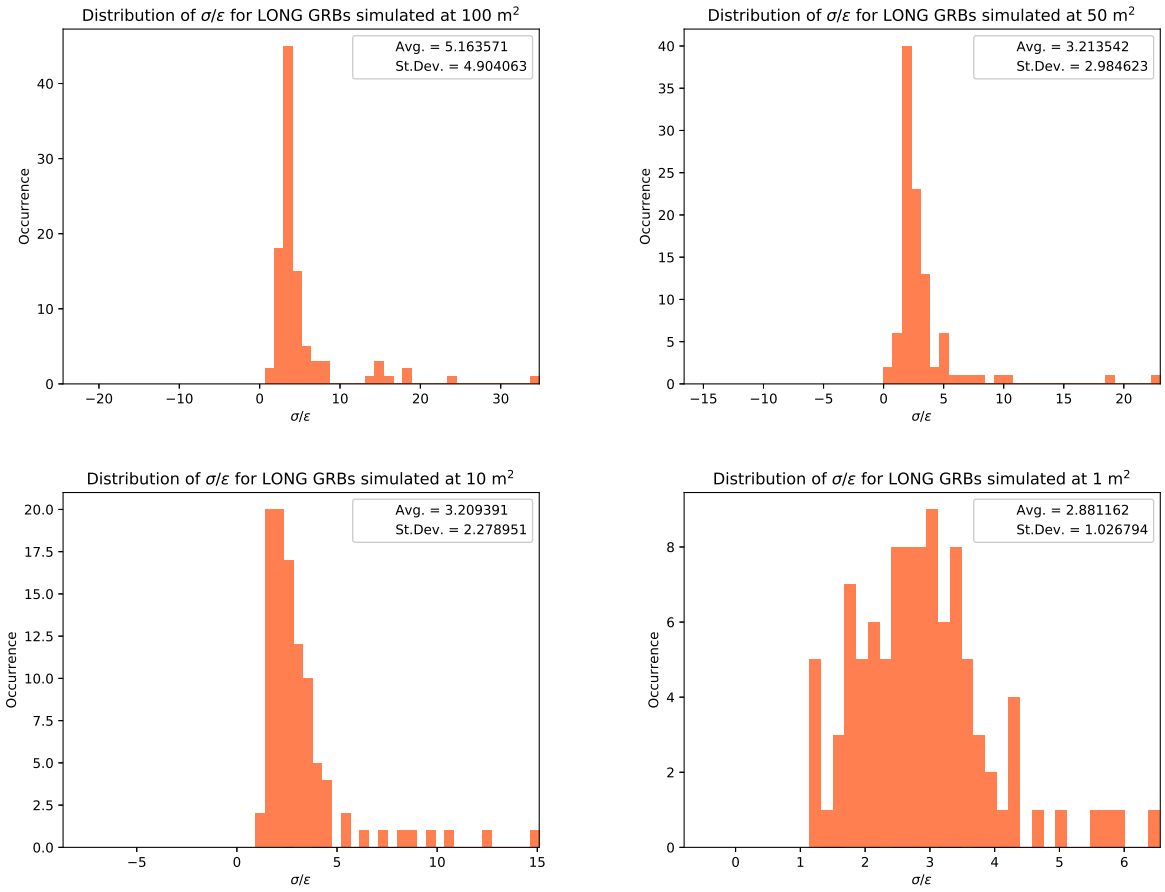

Figure 7. ...

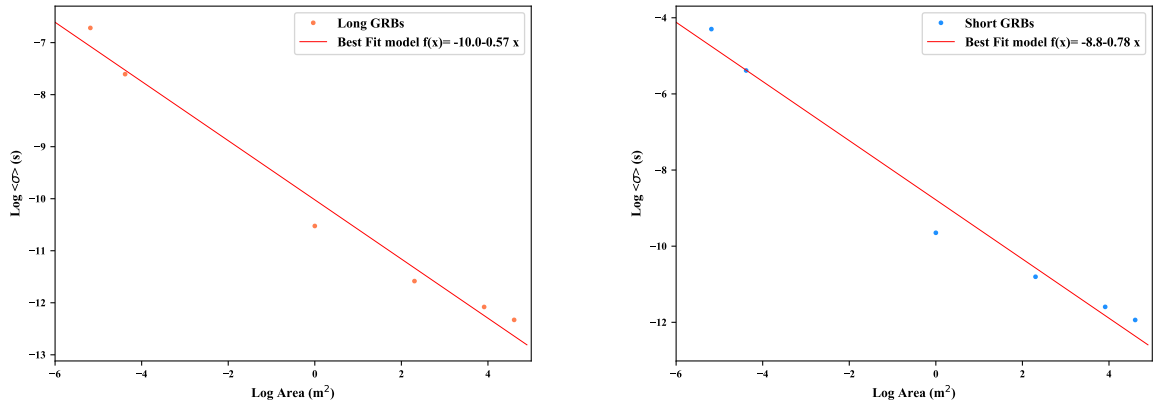

Figure 8. Trend of the mean value of the σ obtained for each simulated area as a function of the area of the detector. We also report the best-fit linear function (red solid line) superimposed in each plot.